



## Phase Relationships in the System Mn-Co-C

Ragnhild E. Aune, Du Sichen and Seshadri Seetharaman

(Received June 16, 1997)

In the present work, phase relationships in the Mn- and Co- rich regions of the Mn-Co-C system have been investigated at 1173 and 1273 K by using an equilibration technique. Alloys of Mn-Co-C were prepared from ultra pure Mn, Co and C powders by mixing the components in required ratios and melting the mixtures in an induction furnace. The melted samples were placed inside quartz capsules and sealed under vacuum. The samples were then placed in the even temperature zone ( $\pm 0.15^\circ\text{C}$ ) of a vertical furnace and heat treated. The duration of the heat treatment was 14 days at 1173 K and 7 days at 1273 K. The samples were quenched in water after heat treatment. The phase identification of the heat treated samples were carried out by SEM (Scanning Electron Microscope), and the chemical analyses of the various phases present were obtained by the EDS (Electron Dispersion Spectroscopy)-detector attached to the SEM-unit.

On the basis of the present results and the phase diagram information for the three binary systems available in literature, the major part of the Mn-Co-C phase diagram at 1173 and 1273 K has been constructed. The results indicate that  $\beta$ -Mn,  $\gamma$ -Mn and  $\alpha$ -Co solid solutions exist over appreciable ranges of composition, and cubic  $(\text{Mn,Co})_{23}\text{C}_6$ , hexagonal  $(\text{Mn,Co})_{15}\text{C}_4$ , monoclinic  $(\text{Mn,Co})_5\text{C}_2$  as well as hexagonal (ortrigonal)  $(\text{Mn,Co})_7\text{C}_3$  occur essentially as line compounds. The various two- and three phase regions existing in this system at the temperatures in question are mapped and the isothermal sections are presented.

### 1. Introduction

Thermodynamics of complex carbides involving transition metals is of great importance for an understanding of the physical metallurgy of steel, as these constituents are the hard second phase that strengthen the steel. As cobalt is an important alloying element in the case of cemented carbides, a study on the thermodynamics of the ternary system Mn-Co-C would be of interest in the field of hard metals.

At the department of Metallurgy, Kungliga Tekniska Högskolan (KTH), Sweden, there is an ongoing program on the systematisation of the thermodynamic data of metal-carbon systems involving transition metals. The following systems have been evaluated at the department:

Mn-C<sup>1</sup>, Cr-C<sup>2</sup>, V-C<sup>3</sup>, and the present aim is to extend these measurements to ternary carbide systems. The work reported in this paper is an experimental study of the equilibria among the several phases of the system Mn-Co-C. While the thermodynamics of the three binaries in the system, *i.e.* Mn-C,<sup>1,4-16</sup> Co-C<sup>17,18</sup> as well as Co-Mn,<sup>17,19-22</sup> are relatively well understood, no similar information is, to the knowledge of the present authors, available in the case of the ternary system.

It may be pointed out at the outset that, in the present work, the various binary and ternary compounds are considered as stoichiometric phases. It is known that carbides in general are not primarily stoichiometric. This, in turn has a significant influence on the thermodynamic properties.

---

Division of Theoretical Metallurgy, Department of Metallurgy, Royal Institute of Technology, S-100 44, Stockholm, Sweden

In view of the experimental complexities and the uncertainties in the measurements involved, it was felt that the scope of the present work may have to be limited by the above assumption.

### 2. Previous Work

The phase diagram of the Mn-C system has been subjected to many experimental investigations.<sup>4-7</sup> Extensive studies of the thermodynamic properties of the system have also been carried out.<sup>8-9</sup> A certain disagreement do exist among the published phase diagrams.<sup>1,10-16</sup> The phase diagram presented in Fig.1 is a combination of the low temperature work by Benz *et al.*<sup>13</sup> and the high temperature results by Schurmann and Geissler.<sup>14</sup> The two parts are connected by dashed lines. As can be seen from the diagram, the compounds included are a hexagonal  $\epsilon$ -phase with a large range of solubility and five carbides ( $Mn_{23}C_6$ ,  $Mn_{15}C_4$ ,  $Mn_3C$ ,  $Mn_5C_2$ ,  $Mn_7C_3$ ) in addition to graphite and phases characteristic of pure Mn ( $\alpha$ ,  $\beta$ ,  $\gamma$ ,  $\delta$  and liquid). Du *et al.*<sup>11</sup> have reexamined the combined phase diagram and their results are indicated in Fig.1 by dot-dash lines. An assessment has also been carried out by Huang<sup>16</sup> based on the experimental phase boundary and thermodynamic data available.

The thermodynamic information regarding the system Co-C is well known. The reviewed phase diagram by Ishida and Nishizawa,<sup>17</sup> presented in Fig.2,

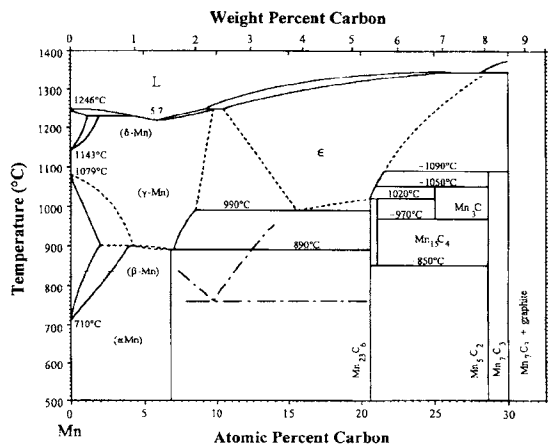


Fig.1 Phase diagram for the binary system Mn-C as proposed by Benz *et al.*,<sup>13</sup> Schurmann and Geissler<sup>14</sup> and Du Sichen *et al.*<sup>11</sup>

is primarily based on the data of Hasebe *et al.*<sup>18</sup> As can be seen from the diagram, the compounds included are graphite and phases characteristic of pure Co ( $\alpha$ ,  $\epsilon$ ).

A thermodynamic assessment of the system Co-Mn has been carried out by Huang.<sup>9</sup> The assessed phase diagram is based on the work of Kaufman,<sup>20</sup> Hasebe *et al.*,<sup>21</sup> and Hillert and Jarl.<sup>22</sup> The reviewed phase diagram by Ishida and Nishizawa<sup>17</sup> is presented in Fig.3. As can be seen from the diagram six phases exist ( $\alpha$ -Co,  $\epsilon$ -Co,  $\alpha$ -Mn,  $\beta$ -Mn,  $\gamma$ -Mn,  $\delta$ -Mn).

The crystal structures (Prototype, Pearson symbol, Strukturbericht designation, Space group) of the binary

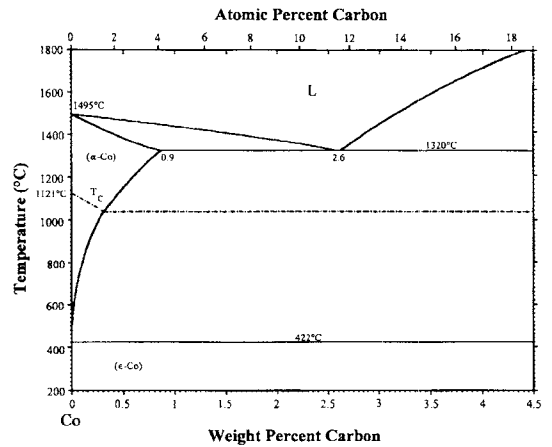


Fig.2 Phase diagram for the binary system Co-C as proposed by Ishida and Nishizawa.<sup>17</sup>

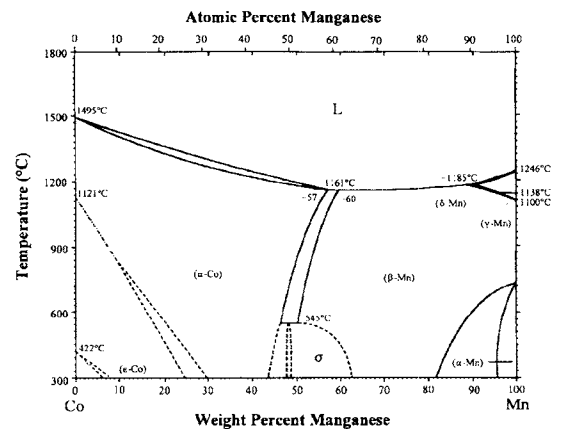


Fig.3 Phase diagram for the binary system Co-Mn as proposed by Ishida and Nishizawa.<sup>17</sup>

**Table 1** Crystal Structures of the phases in the Mn-Co-C system.<sup>7,1</sup>

Phase	C	$\alpha$ -Co	$\epsilon$ -Co	$\epsilon'$ -Co	$\alpha$ -Mn	$\beta$ -Mn	$\gamma$ -Mn	$\delta$ -Mn	Co <sub>3</sub> C	Co <sub>2</sub> C	Mn <sub>23</sub> C <sub>6</sub>	Mn <sub>15</sub> C <sub>4</sub>	Mn <sub>3</sub> C	Mn <sub>5</sub> C <sub>2</sub>	Mn <sub>7</sub> C <sub>3</sub>
Pearson Symbol	<i>hP4</i>	<i>cF4</i>	<i>hP2</i>	....	<i>cI58</i>	<i>cP20</i>	<i>cF4</i>	<i>cI2</i>	<i>oP6</i>	<i>oP6</i>	<i>cF116</i>	....	<i>oP16</i>	<i>mC28</i>	<i>oP40</i>
Space Group	<i>P63/mmc</i>	<i>Fm3m</i>	<i>P63/mmc</i>	....	<i>I43m</i>	<i>P4132</i>	<i>Fm3m</i>	<i>I43m</i>	<i>Pnma</i>	<i>Pnmm</i>	<i>Fm3m</i>	....	<i>Pnma</i>	<i>C2/c</i>	<i>Pnma</i>
Strukturbericht designation	A9	A1	A3	....	A12	A13	A1	A2	D0 <sub>11</sub>	....	D8 <sub>4</sub>	....	D0 <sub>11</sub>	....	D10 <sub>1</sub>
Prototype	Graphite	Cu	Mg	....	$\alpha$ -Mn	$\beta$ -Mn	Cu	W	Fe <sub>3</sub> C	....	Cr <sub>23</sub> C <sub>6</sub>	....	Fe <sub>3</sub> C	....	Cr <sub>7</sub> C <sub>3</sub>

phases of the Mn-Co-C ternary are listed in **Table 1**.

The previous studies on the ternary system have mainly been focusing on the carbon solubility,<sup>23,24</sup> the activity of manganese,<sup>23</sup> the structural and magnetic properties of Mn-Co-C alloys<sup>25</sup> as well as the ferromagnetic structure of Mn<sub>2</sub>Co<sub>2</sub>C.<sup>26</sup>

### 3. Materials, Apparatus, and Procedure

The present work consists of preparing alloys, heat treating the specimens and then examining their structure by using a scanning electron microscope.

#### 3.1 Materials

Alloys of Mn-Co-C were prepared from manganese powder (150  $\mu$ m, MERCK, Germany), cobalt powder (m2N8, Johnson Matthey Alfa Products, Germany) and carbon powder (ultra "F" purity, Ultra Carbon Corporation, U.S.A.). Weighed quantities were obtained by mixing the required ratios of Mn, Co and C powders thoroughly. The mixtures were melted in Al<sub>2</sub>O<sub>3</sub> crucibles placed in graphite enclosers by induction heating. Samples of the alloys were analyzed for C by conventional methods using a  $\mu$ p-controlled automatic analyzer, Rosemount CSA 5003, and the nominal C contents were confirmed within an accuracy of  $\pm 1.5\%$ . No aluminium was detected in the samples during the chemical analysis.

#### 3.2 Apparatus and Procedure

The specimens for microscopic analysis were prepared by placing the samples, together with Al<sub>2</sub>O<sub>3</sub> powder, inside quartz capsules and sealing them under vacuum (0.133 Pa). The samples in the capsules were then sintered in a resistance furnace at desired temperatures for different periods of time, ranging from one week at 1273 K to two weeks at 1173 K. The capsules were placed in the uniform temperature zone of the alumina reaction tube and the temperature was measured by a thermocouple of type S (Pt-10% Rh/Pt) to an accuracy of  $\pm 1$  °C by a Keithley 199 System

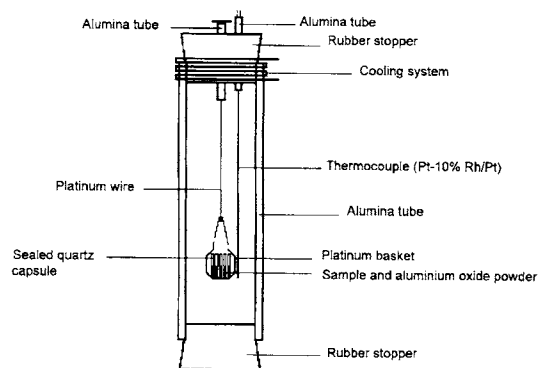


**Fig.4** Schematic diagram of the experimental set-up.

DMM/Scanner. A schematic diagram of the experimental set-up is given in **Fig.4**. After sintering, the samples were quenched by cutting the platinum wire, letting the samples fall into a water bath and breaking them immediately under water. The samples were washed in alcohol, dried and preserved in a desiccator before being analysed. The sintering time for these samples was found to be sufficient for the completion of both the solid- and liquid phase reactions.

The characterization of the annealed alloys was done by metallographic examination. Elemental analysis of the phases present in each alloy was done with a Jeol JSM-840 Scanning Electron Microscope (SEM) connected to an Electron Dispersion Spectroscopy (EDS)-detector, Link AN-10000. The apparatus was calibrated by using spectroscopic standard cobalt. For revealing the microstructure of the alloys, a 4 % nital solution was found most suitable as an etching reagent. The amounts of Co and Mn present in each phase were determined simultaneously by SEM-EDS analysis and recorded as the composition of the phase in at.%. The C content could not be established with a sufficient experimental certainty.

To check the reproducibility of the results obtained

**Table 2** Phase analysis of Mn-Co-C alloys annealed (2 weeks) at 1173 K and quenched in water.

Alloy no.	Nominal composition (at%)			Phase analysis at 1173 K	
	Mn	Co	C	No. of phases	SEM-EDS
1: 1	74.2	1.1	24.6	2 phase	Mn <sub>15</sub> C <sub>4</sub> + Mn <sub>5</sub> C <sub>2</sub>
1: 2	79.4	0.8	19.7	2 phase	$\beta$ -Mn + Mn <sub>23</sub> C <sub>6</sub>
1: 3	84.7	0.8	14.5	3 phase	$\beta$ -Mn + $\gamma$ -Mn + Mn <sub>23</sub> C <sub>6</sub>
1: 4	89.9	0.5	9.5	1 phase	$\gamma$ -Mn
1: 5	94.5	0.8	4.7	2 phase	$\beta$ -Mn + $\gamma$ -Mn
2: 1	67.3	10.3	22.4	2 phase	$\beta$ -Mn + Mn <sub>5</sub> C <sub>2</sub>
2: 2	72.2	9.9	18.0	2 phase	$\beta$ -Mn + Mn <sub>5</sub> C <sub>2</sub>
2: 3	76.9	9.9	13.1	1 phase	$\beta$ -Mn
2: 4	81.6	9.8	8.6	1 phase	$\beta$ -Mn
2: 5	85.6	10.1	4.3	2 phase	$\beta$ -Mn + L
3: 2	64.1	20.0	15.9	2 phase	$\beta$ -Mn + L
3: 3	68.2	20.2	11.6	2 phase	$\beta$ -Mn + L
3: 5	76.1	20.1	3.8	1 phase	$\beta$ -Mn
4: 1	52.3	30.3	17.4	2 phase	$\beta$ -Mn + L
4: 2	55.9	30.1	13.9	2 phase	$\beta$ -Mn + L
4: 3	59.7	30.1	10.2	2 phase	$\beta$ -Mn + L
4: 4	63.5	29.8	6.7	1 phase	$\beta$ -Mn
4: 5	66.7	29.9	3.4	1 phase	$\beta$ -Mn
5: 1	44.4	40.9	14.7	1 phase	$\alpha$ -Co
5: 2	47.4	40.9	11.8	1 phase	$\alpha$ -Co
5: 3	50.7	40.6	8.7	2 phase	$\beta$ -Mn + $\alpha$ -Co
5: 4	53.9	40.4	5.7	1 phase	$\beta$ -Mn

in this work, a couple of samples were sintered and quenched in liquid nitrogen. The elemental analysis of the phases present in these alloys confirmed the earlier findings, thereby confirming the validity of the quenching technique described earlier.

#### 4. Results

The results obtained from the phase analysis of the alloys annealed at 1173 and 1273 K are given in **Table 2** and **3** respectively. The nominal compositions of the alloys in at.% are also listed in these tables.

The mutual consistency between the SEM-EDS results for the various samples confirmed the reliability of the present work. Samples close to the Mn-C binary were in total agreement with the results of Du *et al.*<sup>13</sup> The reliability was further confirmed by repeating some alloy compositions which were close to each other with reproducible results.

The three-phase equilibria ( $\beta$ -Mn +  $\gamma$ -Mn + Mn<sub>23</sub>C<sub>6</sub>) at 1173 K and ( $\beta$ -Mn +  $\epsilon$ -Mn + Mn<sub>23</sub>C<sub>6</sub>) at 1273 K were confirmed by alloy no. 1: 3 (see **Figs.5(a)** and **(b)**). In

**Table 3** Phase analysis of Mn-Co-C alloys annealed (1 weeks) at 1273 K and quenched in water.

Alloy no.	Nominal composition (at%)			Phase analysis at 1273 K	
	Mn	Co	C	No. of phases	SEM-EDS
1: 1	74.2	1.1	24.6	2 phase	Mn <sub>15</sub> C <sub>4</sub> + Mn <sub>3</sub> C
1: 2	79.4	0.8	19.7	2 phase	$\beta$ -Mn + Mn <sub>23</sub> C <sub>6</sub>
1: 3	84.7	0.8	14.5	3 phase	$\beta$ -Mn + $\epsilon$ -Mn + Mn <sub>23</sub> C <sub>6</sub>
1: 4	89.9	0.5	9.5	2 phase	$\gamma$ -Mn + $\epsilon$ -Mn
1: 5	94.5	0.8	4.7	2 phase	$\beta$ -Mn + $\gamma$ -Mn
2: 1	67.3	10.3	22.4	2 phase	Mn <sub>7</sub> C <sub>3</sub> + L
2: 2	72.2	9.9	18.0	1 phase	$\beta$ -Mn
2: 3	76.9	9.9	13.1	2 phase	$\beta$ -Mn + L
2: 4	81.6	9.8	8.6	2 phase	$\beta$ -Mn + L
2: 5	85.6	10.1	4.3	2 phase	$\beta$ -Mn + L
3: 1	59.9	20.3	19.9	2 phase	$\beta$ -Mn + L
3: 2	64.1	20.0	15.9	2 phase	$\beta$ -Mn + L
3: 3	68.2	20.2	11.6	2 phase	$\beta$ -Mn + L
3: 4	72.3	20.1	7.7	1 phase	$\beta$ -Mn
3: 5	76.1	20.1	3.8	1 phase	$\beta$ -Mn
4: 1	52.3	30.3	17.4	2 phase	$\beta$ -Mn + L
4: 2	55.9	30.1	13.9	2 phase	$\beta$ -Mn + L
4: 3	59.7	30.1	10.2	1 phase	$\beta$ -Mn
4: 4	63.5	29.8	6.7	1 phase	$\beta$ -Mn
4: 5	66.7	29.9	3.4	1 phase	$\beta$ -Mn
5: 1	44.4	40.9	14.7	1 phase	$\alpha$ -Co
5: 2	47.4	40.9	11.8	2 phase	$\beta$ -Mn + $\alpha$ -Co
5: 3	50.7	40.6	8.7	2 phase	$\beta$ -Mn + $\alpha$ -Co
5: 4	53.9	40.4	5.7	1 phase	$\beta$ -Mn
5: 5	56.7	40.5	2.9	1 phase	$\beta$ -Mn

**Fig.5(a)** the white phase regions correspond to the  $\beta$ -Mn phase. Light gray regions and dark gray regions correspond to the  $\gamma$ -Mn and Mn<sub>23</sub>C<sub>6</sub> phases respectively. In **Fig.5(b)** the white phase regions also correspond to the  $\beta$ -Mn phase. Light gray regions and dark gray regions correspond to the  $\epsilon$ -Mn and Mn<sub>23</sub>C<sub>6</sub> phases respectively.

The phase relations in the system, at both temperatures, are also characterized by the existence of a liquid area. It is a well known fact that when the solubility of C in a phase increases, the melting point of that phase decreases. With this in mind, and the fact that a liquid phase is formed above 1433 K in the binary system Co-Mn, it could be expected that a liquid phase in the Mn-Co-C ternary system may occur at a lower temperature. The two-phase equilibrium ( $\beta$ -Mn + liquid) was confirmed by alloy no. 2: 5, 3: 2, 3: 3, 4: 1, 4: 2 and 4: 3 at 1173 K and alloy no. 2: 3, 2: 4, 2: 5, 3: 1, 3: 2, 3: 3, 4: 1 and 4: 2 at 1273 K. In **Fig.6**

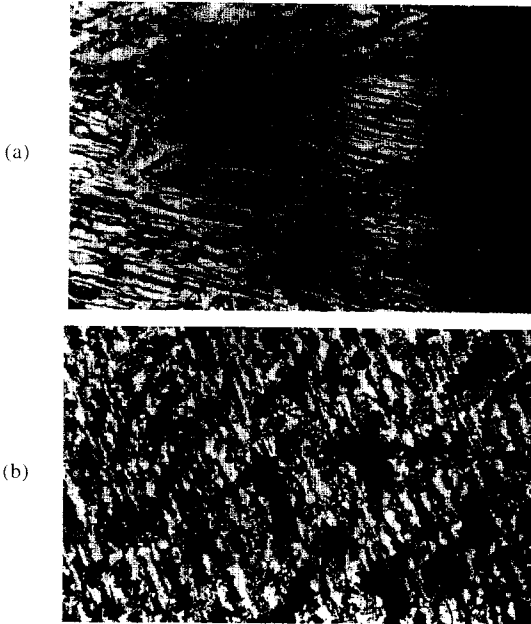


**Fig.5** Microstructure of alloy no. 1:3, with the nominal composition: (at.%Mn) = 84.7, (at.%Co) = 0.8, annealed at 1173 K for 2 weeks and 1273 K for 1 week (etched in 4% nital solution; optical micrograph; magnification 200 times).

(a) Observed phases at 1173 K: ( $\beta$ -Mn +  $\gamma$ -Mn +  $Mn_{23}C_6$ ). The white phase regions correspond to  $\beta$ -Mn. Light gray regions and dark gray regions correspond to  $\gamma$ -Mn and  $Mn_{23}C_6$  respectively.  
 (b) Observed phases at 1273 K: ( $\beta$ -Mn +  $\epsilon$ -Mn +  $Mn_{23}C_6$ ). The white phase regions correspond to  $\beta$ -Mn. Light gray regions and dark gray regions correspond to  $\epsilon$ -Mn and  $Mn_{23}C_6$  respectively.

the structure of alloy no. 2:4 at 1273 K is presented. As can be seen from the figure two different structural modifications exist. The white phase regions correspond to the  $\beta$ -Mn phase and the gray regions to the liquid phase.

The two-phase equilibrium ( $\beta$ -Mn +  $\alpha$ -Co) was confirmed by alloy no. 5:3 at 1173 K and no. 5:2 and 5:3 at 1273 K (see **Figs.7**(a) and (b)). In **Figs.7**(a) and (b), the white phase regions correspond to the  $\beta$ -Mn phase and the gray regions correspond to the  $\alpha$ -Co phase. One of the differences between the two diagrams is the stability of this two-phase equilibrium, which appears at different composition ranges.



**Fig.6** Microstructure of alloy no. 2:4, with the nominal composition: (at.%Mn)=81.6, (at.%Co)=9.8, annealed at 1273 K for 1 week (etched in 4% nital solution; optical micrograph; magnification 200 times). Two different structural modifications exist. Observed phases: ( $\beta$ -Mn + liquid). The white phase regions correspond to the  $\beta$ -Mn phase and the gray regions to the liquid phase.

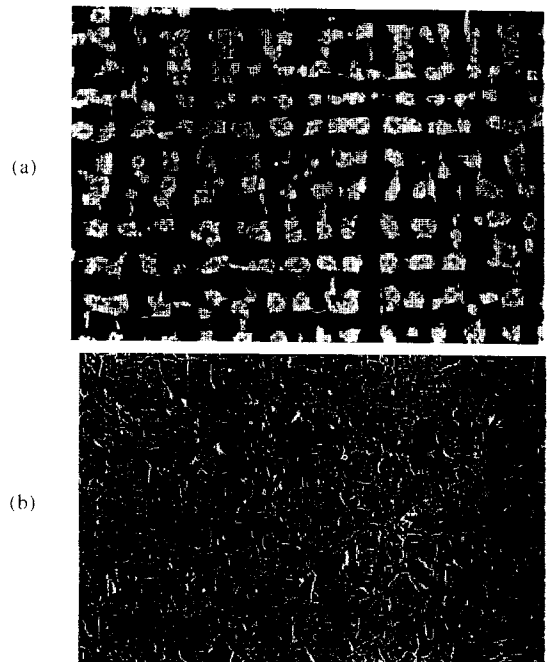


**Fig.7** Microstructure of alloy no. 5:3, with the nominal composition: (at.%Mn)=50.7, (at.%Co)=40.6 annealed at 1173 K for 2 weeks and 1273 K for 1 week (etched in 4% nital solution; optical micrograph; magnification 200 times). (a) and (b). Observed phases at 1173 K and 1273 K: ( $\beta$ -Mn +  $\alpha$ -Co). The white phase regions correspond to the  $\beta$ -Mn phase and the gray regions

### 5. Discussion

All the phases observed in the Mn-Co-C system, at 1173 and 1273 K, have been identified to be extensions of the phases found in the binary systems. They are  $\beta$ -Mn,  $\gamma$ -Mn,  $\epsilon$ -Mn,  $Mn_{23}C_6$ ,  $Mn_{15}C_4$ ,  $Mn_3C$ ,  $Mn_5C_2$ ,  $Mn_7C_3$ ,  $\alpha$ -Co and liquid.

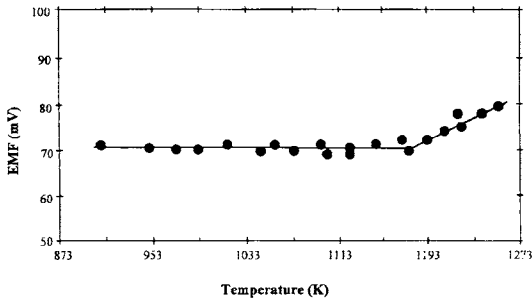


**Fig.8** EMF (electromotive force) vs. temperature for the galvanic cell:  $Mn, MnF_2, CaF_2 || CaF_2 || CaF_2, MnF_2, Mn_7C_3, graphite$  (+)

The five carbides,  $Mn_{23}C_6$ ,  $Mn_{15}C_4$ ,  $Mn_3C$ ,  $Mn_5C_2$  and  $Mn_7C_3$ , have in the present work been treated as liner compounds. A similar treatment was adopted by Benz *et al.*<sup>27)</sup> in their thermodynamic study of the solid phases in the system Fe-Mn-C and by Huang<sup>28)</sup> in her thermodynamic assessment of the Fe-Mn-C system. Limited ranges of Co solubility, less than 3.2 at.% in the  $Mn_{23}C_6$ ,  $Mn_{15}C_4$ ,  $Mn_5C_2$  and  $Mn_7C_3$  phases at 1173 K and less than 2.4 at.% in the  $Mn_{23}C_6$ ,  $Mn_{15}C_4$ ,  $Mn_5C_2$ ,  $Mn_3C$  and  $Mn_7C_3$  phases at 1273 K, were detected within experimental uncertainty.

As mentioned in the introduction, the agreement among the published binary phase diagrams of the Mn-C system<sup>1, 10-16)</sup> is only qualitative. Du *et al.*<sup>1)</sup> found much higher carbon solubility in the  $\gamma$ -Mn phase than the earlier investigators (see Fig.1). A number of attempts were made by Du *et al.*<sup>1)</sup> to obtain the high temperature  $\gamma$ -Mn phase, but due to serious experimental difficulties no conclusive evidence could be obtained. This was, according to Du *et al.*,<sup>1)</sup> due to

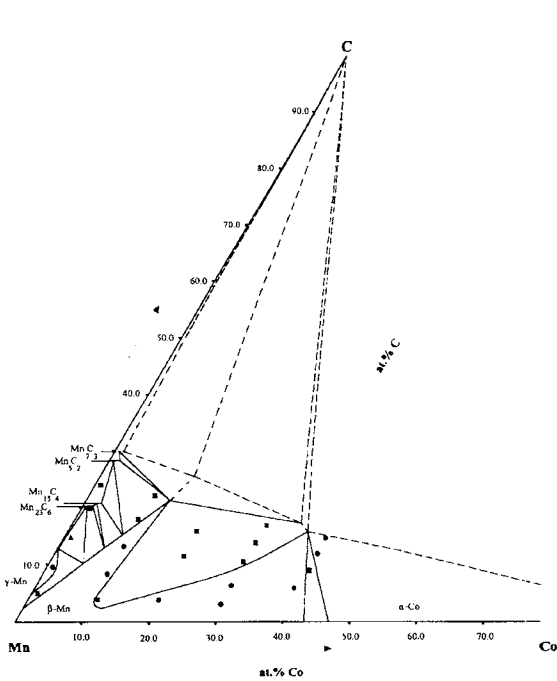


**Fig.9** Isothermal section the Mn-Co-C system at 1173 K. The symbols show the phases observed at room temperature: ● single-phase, ■ two-phase, ▲ three-phase.

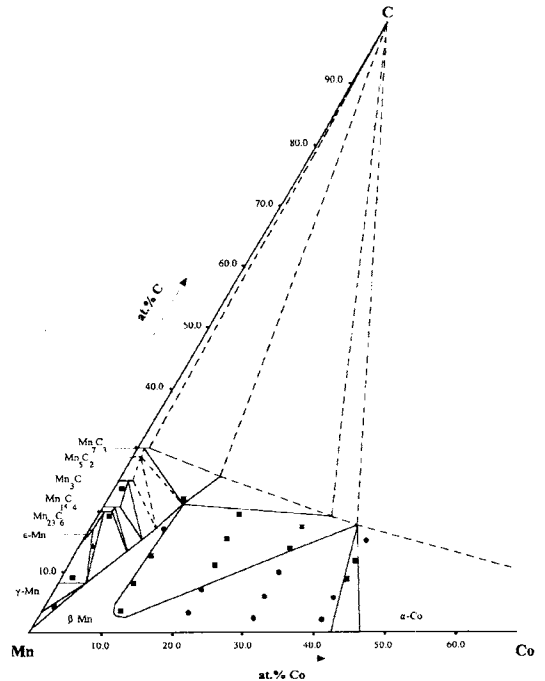


**Fig.10** Isothermal section the Mn-Co-C system at 1273 K. The symbols show the phases observed at room temperature: ● single-phase, ■ two-phase, ▲ three-phase.

the phase transformations involved being very fast. The same difficulties seem to have been faced by many of the earlier investigators.<sup>11, 13, 29-31</sup> It was proposed by Du *et al.*<sup>11</sup> that if the  $\gamma$ -Mn phase present at high temperatures got converted to  $\alpha$ -Mn by means of a diffusionless transformation, a sample in the  $\gamma$ -Mn single-phase region at high temperature is likely to result in a single  $\alpha$ -Mn phase. This hypothesis was later verified by Du *et al.*<sup>11</sup> Huang,<sup>16</sup> on the other hand, gave this data a very low weight in her thermodynamic assessment of the Mn-C system. In the present work, however, the existence of such a phase was confirmed by alloy no. 1:4 at 1173 K which was located in this region.

Another interesting feature observed earlier by Du *et al.*<sup>32</sup> in their galvanic cell measurements using the cell:

(-)Mn, MnF<sub>2</sub>, CaF<sub>2</sub> || CaF<sub>2</sub> || CaF<sub>2</sub>, MnF<sub>2</sub>, Mn<sub>7</sub>C<sub>3</sub>, graphite(+)

(the cell reaction being:  $7\text{Mn} + 3\text{C} \rightleftharpoons \text{Mn}_7\text{C}_3$ ) was the

existence of a distinct break in the EMF (electromotive force) vs. temperature relationship obtained in this work at 1181 K. The figure illustrating this provided by these authors is reproduced in Fig.8. A possible transformation of graphite at 1181 K has not been evidenced in the EMF measurements of Jacob and Seetharaman.<sup>33</sup> Du *et al.*<sup>32</sup> have attributed this break to the possible formation of a new phase between Mn<sub>7</sub>C<sub>3</sub> and graphite. Attempts were made in the present work to investigate this phase relation, but with inconclusive results. Further work is ongoing in this regard.

During the elemental analysis of the alloys no evidence was found for the existence of any ternary intermediate phase. Alloy no. 5:1 (with the nominal composition (at.% Mn)=44.4 and (at.% Co)=40.9) is located close to the composition of compound Mn<sub>2</sub>Co<sub>2</sub>C; but no conclusive evidence was found in this alloy for the existence of this phase at the temperatures in question. As no alloy was prepared exactly at the right composition, further work must be conducted in this region to exclude the uncertainty as to its existence.

Isothermal sections for the system Mn-Co-C at 1173 and 1273 K have been drawn from the results obtained in this present work and are shown in Figs.9 and 10 respectively. The isothermal sections were constructed using tie line and tie triangle data. The equilibria that were not confirmed experimentally are

indicated by dashed tie-lines. Phase boundaries on the binary sides of each isothermal section were taken from the respective binary systems. The unexplored portions of the ternary systems are sketched only tentatively in the figures and are based on the respective binary phase diagrams. All the alloy compositions that were analyzed are also shown in the figures (located at the nominal composition of the alloy).

The present results can be combined with the thermodynamic data available for the ternary as well as the lower-order systems to arrive at a comprehensive description of the Mn-Co-C ternary by the so-called CALPHAD approach.<sup>34</sup> Such efforts are currently in progress.

## 6. Summary of Result

Alloys of a wide range of compositions in the system Mn-Co-C were quenched in water after prolonged anneals at 1173 and 1273 K. The resulting phases and structures were studied by using a scanning electron microscope. Isothermal phase diagrams at 1173 and 1273 K are shown. The diagrams are consistent with previously determined binary phases reported in the literature. The existence of a  $\gamma$ -Mn phase, in the Mn-C binary system, with a higher carbon solubility was confirmed at 1173 K. No ternary compound was found, and only limited solubility was measured in the constituent binary phases. Measured solid solubilities of Co were less than 3.2 at.% at 1173 K in the following phases: Mn<sub>23</sub>C<sub>6</sub>, Mn<sub>15</sub>C<sub>4</sub>, Mn<sub>5</sub>C<sub>2</sub>, Mn<sub>7</sub>C<sub>3</sub> and less than 2.4 at.% at 1273 K in Mn<sub>23</sub>C<sub>6</sub>, Mn<sub>15</sub>C<sub>4</sub>, Mn<sub>5</sub>C<sub>2</sub>, Mn<sub>3</sub>C and Mn<sub>7</sub>C<sub>3</sub>. The existence of the ( $\beta$ -Mn +  $\gamma$ -Mn + Mn<sub>23</sub>C<sub>6</sub>) (1173 K) and ( $\beta$ -Mn +  $\epsilon$ -Mn + Mn<sub>23</sub>C<sub>6</sub>) (1273 K) three-phase regions were also confirmed together with the two-phase equilibrium ( $\beta$ -Mn +  $\alpha$ -Co) (1173 and 1273K) and a liquid area (1173 and 1273 K). Several micro-structures are illustrated by photomicrographs.

**Acknowledgements:** The authors wish to acknowledge the assistance of Mr. Istvan Varga with the experimental equipment and the help and valuable guidance of Mr. Nils Lange in carrying out the microscopic examinations. The investigation was supported by the Swedish Research Council for Engineering Sciences (TFR).

## References

- 1) Du Sichen, S. Seetharaman and L. I. Staffansson,

- Metall. Trans. B* **20B**, 747 (1989).
- 2) Du Sichen, S. Seetharaman and L. I. Staffansson. *Metall. Trans. B* **20B**, 911 (1989).
  - 3) Du Sichen, *Metall. Trans. B* **21B**, 313 (1990).
  - 4) M. Hansen and K. Anderko, Constitution of Binary Alloys, McGraw-Hill, New York (1958).
  - 5) R. P. Elliott, Constitution of Binary Alloys, 1st suppl., McGraw-Hill, New York (1965).
  - 6) F. A. Shunk, Constitution of Binary Alloys, 2nd suppl., McGraw-Hill, New York (1969).
  - 7) T. B. Massalski, Binary Alloy Phase Diagrams, American Society for Metals, Metals Park, OH, (1986).
  - 8) R. Hultgren, P. D. Desai, D. T. Hawkins, M. Gleiser and K. K. Kelley, Selected Values of Thermodynamic Properties of Binary Alloys, American Society for Metals, Metals Park, OH (1973).
  - 9) M. Hillert and M. Waldenström, *Metall Trans. A* **8A**, 5 (1977).
  - 10) R. Vogel and W. Doring, *Arch Eisenhüttenwes.* **9**, 247 (1935).
  - 11) M. Isobe, *Sci. Rep. Res. Tohoku. Univ. A* **3**, 468 (1951).
  - 12) H. Schenck, M. G. Froberg and E. Steinmetz, *Arch. Eisenhüttenwes.* **34**, 37 (1963).
  - 13) R. Benz, J. F. Elliot and J. Chipman, *Metall. Trans.* **4**, 1449 (1973).
  - 14) E. Schumann and I. K. Geissler, *Giesserei-Forsch.* **29**, 153 (1977).
  - 15) A. Tanaka, *Trans. Jpn. Inst. Met.* **20**, 516 (1979).
  - 16) W. Huang, *Scand. J. Metallurgy* **19**, 26 (1990).
  - 17) K. Ishida and T. Nishizawa, ASM Handbook, Vol. 3. Alloy Phase Diagrams ASM International, Materials Park, OH (1992).
  - 18) M. Hasebe, H. Ohtani and T. Nishizawa, *Metall. Trans. A* **16A**, 913 (1985).
  - 19) W. Huang, *Calphad* **13**, 231 (1989).
  - 20) L. Kaufman, *Calphad* **2**, 117 (1978).
  - 21) M. Hasebe, K. Oikawa and T. Nishizawa, *J. Jpn. Inst. Met.* **46**, 577 (1982).
  - 22) M. Hillert and M. Jarl, *Calphad* **2**, 227 (1978).
  - 23) C. Petot and P. Desré, *Comptes Rendus, Série C.* **t.264**, 281 (1967).
  - 24) W. L. Daines and R. P. Pehlke, *Transactions of the ASM* **57**, 1011 (1964).
  - 25) A. H. Holtzman and G. P. Conrad, *J. Applied Physics*, supplement to Vol. 30, 103S (1959).
  - 26) N. S. Satya Murthy, R. J. Begum, C. S. Somanathan, B. S. Srinivasan and M. R.L. N. Murthy, *J. Phys. Chem. Solids.* **30**, 939 (1969).
  - 27) R. Benz, J. F. Elliot and J. Chipman, *Metall. Trans.* **4**, 1975 (1973).
  - 28) W. Huang, *Metall. Trans. A* **21A**, 2115 (1990).
  - 29) K. Kuo and L.E.Persson, *J. Iron Steel Inst.* **178**, 39 (1954).
  - 30) J. P. Bouchaud, *Ann. Chim., Ser.* **14[2]**, 353 (1967).
  - 31) P. Lesage, *Ann. Chim. Ser.* **13[6]**, 623 (1961).
  - 32) Du Sichen, S. Seetharaman and L. I. Staffansson, *Metall. Trans. B* **19B**, 951 (1988).
  - 33) K. T. Jacob and S. Seetharaman, *Metall. and Mater. Trans. B* **25B**, 149 (1994).
  - 34) R. E. Aune, S. Sridhar and Du Sichen, *J. Chem. Thermodynamics* **26**, 493 (1994).